HYDRAULIC MODEL OF A NEW BIPOLAR CELL FOR ALUMINUM PRODUCTION①

Gao Zhaosheng, Li Guoxun, Shen Jianyun
Beijing General Research Institude for Nonferrous Metals, Beijing 100088

ABSTRACT The electrolyte circulations in monopolar cell and two-compartment bipolar cell with submerged electrodes were described by a hydraulic model. The influence of current density, electrode tilt, anode-cathode distance (ACD) and immersion depth of electrodes on the electrolyte circulation velocities between electrodes had been studied. Results demonstrated that the flow rates in the two compartments of bipolar cell were very different, which provided important information for the structure design of bipolar cell.

Key words aluminum electrolysis hydraulic model bipolar cell

1 INTRODUCTION

With further development of aluminum electrolysis technology and understanding of this process, today the defects of electrolytic cell with single compartment, that is, lower voltage efficiency and productivity per unit equipment, are exposed more and more obviously, while the cell with inert cathode or bipolar cell gains by contrast. Grjotheim K and Jarrett N *et al*[1-3] recently pointed out that the ultimate aluminum electrolysis cell would have bipolar electrodes using Al_2O_3 as the raw material.

In the past, much attention was only focussed on the material corrision and electrolyte composition[4-9]. Recently, Yang J H *et al*[10] did some work on the current lose besides on electrode materials. However, how to solve another important problem concerning the fluid dynamics and how to design the electrodes and structure of bipolar cell have not been reported. Since a better electrolyte circulation in the cell should give each compartment equivallent concentration of dissolved alumina, especially for a bipolar multi-compartment cell, the present paper studied this

2 THE HYDRAULIC MODEL

As the temperature in practical electrolytic process is high, it is difficult to operate and measure. The present study on transport phenomena and some dynamic processes was based on a physical model, with water as simulated electrolyte, and for the need of measurment, a little amount of $K_4Fe(CN)_6$, $K_3Fe(CN)_6$(0.01 mol/L) and NaOH was added. In order that the model reflects practical process, the geometric and dynamic similarities must be fulfilled. Here the compressed air passing through the holes of electrodes was used to simulate the anode gas to ensure the dynamic similarity[11].

The model cell consisted of glass container whose inner dimensions were 330 mm long, 170 mm wide and 250 mm high, The bipolar electrode and end-anode were made of plexiglass of 4 mm thick with outer size of 250 mm $\times$ 170 mm $\times$ 25 mm. There were many holes at the bottom of the electrodes (about 4 holes/cm^2, d = 0.5 mm); end-cathode was a glass plate. Considering that in this type of bipolar cell with inert electrodes, liquid aluminum would not accumulate on the cathode and the

metallic phase and magnetic field were simulated in this test.

According to Ref. [9,13], there were two kinds of electrode arrays in bipolar cell, see Fig. 1. Some recent research results[14] showed that when the electrodes were in vertical configuration, the liberated bubbles would disperse near the top-quarter anode, which might lead to reoxidation of aluminum formed on the cathode; while the horizontal configuration could give rise to better electrolyte circulations. So, type (b) was selected. Moreover, the inert electrodes could not be easily manufactured into various complex shapes, plate electrode with no grooves was used here.

3 EXPERIMENTS

The equipments used included the small air compressor, rotameter, electrochemical probe, coordinatometer, A/D converter, microcomputer, ruler, etc. The experimental apparatus is shown in Fig. 2.

Electrochemical probe fastened to a three dimensional coordinatometer was used to measure bath flow rate[15]. The flow rates in the center of anode-cathode distance (ACD) were measured in this test and 15 points which were one centimeter away from each other were measured along the width direction. It was found that the velocity distribution was uniform, and the average value was taken as the center velocity of ACD. The probe could move in three directions, so velocities at different points could be measured.

4 RESULTS AND DISCUSSION

According to the mass conservation law of the reaction, the following relation of gas formation rate and current density can be deduced:

$$q = iRT/4Fp$$

The changes in current density were simulated by varying the air flow rate.

4.1 *Comparison of the Behaviors of Two Multi-hole Electrode Plates*

In order to avoid the effect caused during the manufacture of the plates on the experi -

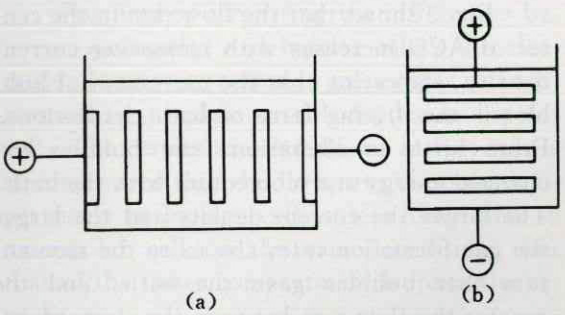

Fig. 1 Plot of bipolar cell models
(a)—vertical configuration;
(b)—horizontal configuration

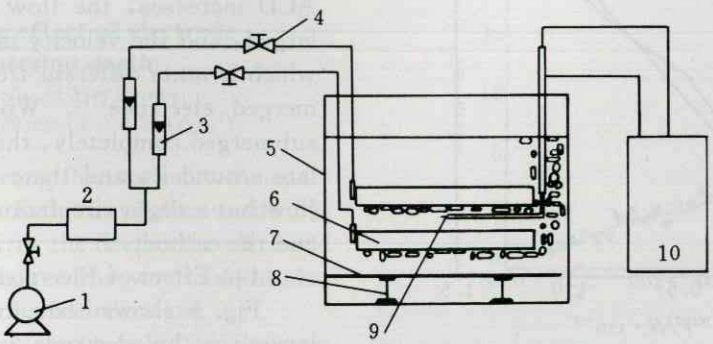

Fig. 2 Sketch of the experimental apparatus
1—air compressor; 2—voltage stabilizer; 3—rotameter; 4—throttle;
5—model cell; 6—bipolar or end-anode; 7—end-cathode;
8—electrode tilt adjuster; 9—electrochemical probe; 10—data acquisition system

ment results, the behaviors of the two multi-hole electrode plates were studied in a monopolar cell. Results are shown in Fig. 3. Their behaviors were nearly the same, and both of their bubbles were liberated uniformly from the bottom of the electrode plates, therefore on the same conditions, the two plates could simulate the same process.

4.2 *Experiment in Monopolar Cell*

Because the structure of multi-compartment cell is more complex, simulation experiments were usually carried out in monopolar cell. So, here the simulations were first done in monopolar cell and compared with the results in literatures to evaluate the correctness of our models, and then they would be extended to multi-compartment cells.

(1) The Influence of Current Density

Fig. 3 shows that the flow rate in the center of ACD increases with increasing current density, indicating that the movement of bubbles is the driving force of bath circulations. From birth to liberation, the bubbles exchanged energy and momentum with the bath. The larger the current density and the larger the gas formation rate, the more the momentum that bubbles gave the bath, and the greater the flow rate between the electrodes.

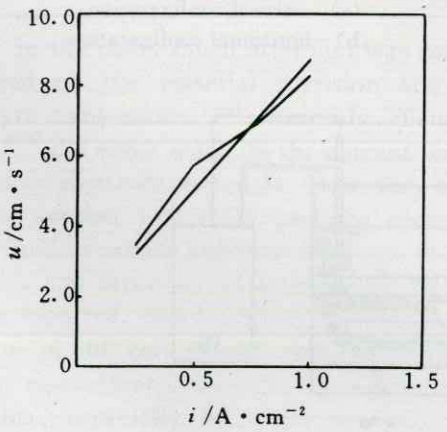

Fig. 3 Comparison of behaviors of two multi-hole electrode plates

($\alpha = 5°$; $H = 30$ mm; ACD = 30 mm; $W_1 = W_2 = 30$ mm)

(2) The Influence of Electrode Tilt

Fig. 4 illustrates that the flow rate increases as the electrode tilt increases, for the bubbles are accelerated by the buoyance along the electrode plate which equals $(\rho-\rho_g)g\sin\alpha$ and increases with the increasing tilt α. In the case of larger tilt α, the bubbles gain more momentum, and the flow rate in the middle of ACD becomes larger.

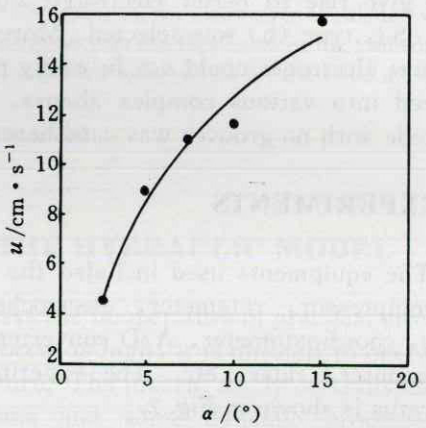

Fig. 4 Influence of electrode tilt on bath flow rate

(ACD = 25 mm; $W_1 = W_2 = 30$ mm; $i = 0.5$ A/cm^2; $H = 25$ mm)

(3) The Effect of ACD

Fig. 5 shows that the flow rate decreases as the ACD increases, indicating that the results fulfill the continuity equation. As the ACD increases, the flow area would be enlarged, and the velocity might become small, which is quite different from that of non-submerged electrode[11]. When an electrode is submerged completely, the bath can not circulate around it, and there is no unidirectional flow but a slight circulation between the anode and the cathode.

(4) Effect of Electrode Immersion Depth

Fig. 6 shows that the velocity becomes larger as the electrode immersion depth increases. This is related to the wave amplitude induced by the liberation of bubbles from the surface of the electrodes. Because the bath fluctuation needs energy, when the wave am-

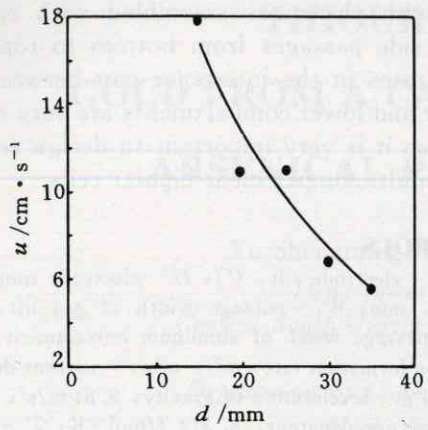

Fig. 5 The relationship between flow rate and ACD(d)
($\alpha = 7.5°$; $W_1 = W_2 = 30$ mm; $H = 25$ mm; $i = 0.5$ A/cm^2)

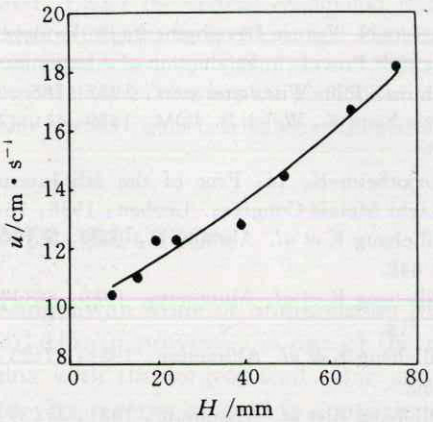

Fig. 6 The effect of electrode immersion depth
($\alpha = 7.5°$; ACD = 25 mm; $W_1 = W_2 = 20$ mm; $i = 0.5$ A/cm^2)

plitude is larger(strong fluctuation), the energy accelarating the bath circulation would become less. Therefore, the deeper the electrode immersion, the slighter the wave amplitude, then the better the bath circulation.

(5) The Flow Rate Distribution Between the Anode and the Cathode

Since bath circulation would affect removing aluminum from the cathode, the flow rate was measured between the anode and the cathode. As shown in Fig. 7, the flow rate near the anode surface is the largest, and that near the cathode the smallest. This is beneficial to the drainage of bubbles and the entrainment of aluminum along the opposite direction; in addition there is density difference between electrolyte and liquid aluminum, so it will present no problem to separate aluminum from the bath.

4.3 *Bath Circulation in Bipolar Cell*

The bath flow rate of each compartment in bipolar cell was measured at different current density. The results are plotted in Fig. 8. It can be seen that the flow rate of the lower compartment is much greater than that of the upper one. After having exchanged the electrode positions and tested many times, we got the same results.

For further comparing the differences between monopolar and bipolar cells, the electrode plates were tested in monopolar cell corresponding to their actual depths in bipolar cell. The results are also shown in Fig. 8. It is demonstrated that the flow rate of upper compartment in bipolar cell is less than that in monopolar cell on the same condition, but that of the lower compartment is quite the reverse.

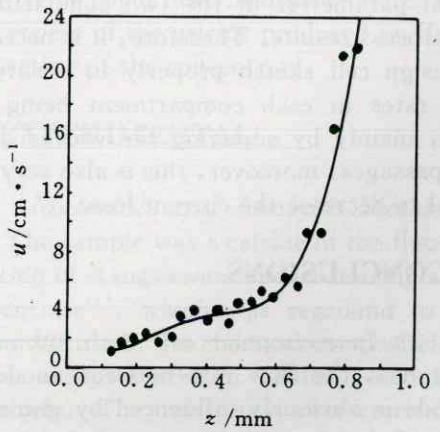

Fig. 7 Variation of flow rates between the anode and the cathode
($\alpha = 5°$; $W_1 = W_2 = 30$ mm; ACD = 30 mm; $H = 40$ mm)

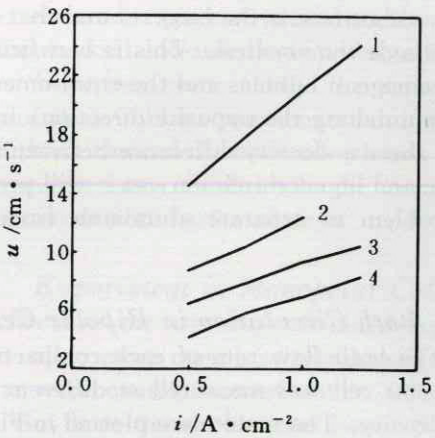

Fig. 8 Comparison of the flow rates in two compartments of bipolar cell with that of monopolar cell

($\alpha = 10°$; ACD = 30 mm; $W_1 = W_2 = 30$ mm; $H = 30$ mm)

1, 4—measured velocities in the lower and upper compartments of bipolar cell;

2, 3—corresponding velocities in the lower and upper compartments of monopolar cell

4.4 *Discussion*

From the experimental results, it is clear that, if electrodes were arrayed with equally wide side passages, the bath flow rates would be very different in both compartments, which would have influence on the control of technological parameters of the two compartments and process results. Therefore, it is necessary to design cell sketch properly to ensure the flow rates in each compartment being uniform, mainly by adjusting the widths of the side passages; moreover, this is also very beneficial to decrease the current loss.

5 CONCLUSIONS

(1) In monopolar cell with submerged electrodes, the flow rate between anode and cathode is obviously influenced by immersion depth of the electrodes.

(2) The bath flow rate distribution, which is beneficial to the liberation of bubbles and the drainage of aluminum, is very rational in our model cell.

(3) It is demonstrated that in the bipolar cell with electrodes assembled with equally wide side passages from bottom to top, the flow rates in the interpolar gap between the upper and lower compartments are very different, so it is very important to design reasonable multi-compartment bipolar cells.

SYMBOLS

α —electrode tilt, (°); H —electrode immersion depth, mm; W_1 —passage width of gas lift, mm; W_2 —passage width of aluminum entrainment, mm; q —gas formation rate, $m^3/s \cdot m^2$; i —current density, A/m^2; g —acceleration of gravity, 9.81 m/s^2; R —universal gas conatant, 8.314 J/mol · K; T —Kelvin temperature, K; F —Faraday constant, 96 500 C/mol; p —pressure, Pa; ρ —density of electrolyte, g/m^3; ρ_g —density of gas, kg/m^3; z —distance from anode, mm; μ —bath flow rate, cm/s.

REFERENCES

1 Jarrett N. Future Developments in the Bayer-Hall-Heroult Process in Production of Aluminum and Alumina. John Wiley and sons, 1987: 188—207.

2 Grjotheim K, Welch B. JOM, 1989, 41(11): 12—16.

3 Grjotheim K. In: Proc of the 8th International Light Metals Congress. Leoben: 1988: 76—81.

4 Billehaug K *et al.* Aluminum, 1980, 56(10): 642—648.

5 Billehaug K *et al.* Aluminum, 1980, 56(11): 713—718.

6 Billehaug K *et al.* Aluminum, 1981, 57(2): 146—150.

7 Billehaug K *et al.* Aluminum, 1981, 57(3): 228—231.

8 Schmidt-Hatting W *et al.* US 3 578 580. 1971.

9 Alder H. US 3 930 967. 1976.

10 Yang Jianhong. PhD Thesis (in Chinese). Central South University of Technology, 1992.

11 Solheim A *et al.* In: Proc of the 118th AIME Annual Meeting. Warrendale, PA: TMS-AIME, 1989: 245—252.

12 Lacamera A F. In: Proc AIME Conf. 1987: 671—691.

13 De Varda G. US 3 554 893. 1971.

14 Shekhar R, Evans J W. In: Proc of the 119th AIME Annual Meeting. Warrendale, PA: TMS-AIME, 1990: 243—248.

15 Gao Zhaosheng *et al.* Nonferrous metals, 1995, (2): 39—41.

(Edited by Li Jun)